World Journal of Microbiology and Biotechnology (2018) 34:10
https://doi.org/10.1007/s11274-017-2383-6

ORIGINAL PAPER

Cloning, purification and characterization of novel Cu-containing nitrite reductase from the *Bacillus firmus* GY-49

Haofeng Gao[1] · Caiqing LI[1] · Bandikari Ramesh[2] · Nan Hu[1]

Received: 31 March 2017 / Accepted: 22 November 2017 / Published online: 18 December 2017

Abstract
Nitrite is generated from the nitrogen cycle and its accumulation is harmful to environment and it can be reduced to nitric oxid by nitrite reductase. A novel gene from *Bacillus firmus* GY-49 is identified as a *nirK* gene encoding Cu-containing nitrite reductase by genome sequence. The full-length protein included a putative signal peptide of 26 amino acids and shown 72.73% similarity with other Cu-containing nitrite reductase whose function was verified. The 993-bp fragment encoding the mature peptide of NirK was cloned into pET-28a (+) vector and overexpressed as an active protein of 36.41 kDa in the *E.coli* system. The purified enzyme was green in the oxidized state and displayed double gentle peaks at 456 and 608 nm. The specific activity of purified enzyme was 98.4 U/mg toward sodium nitrite around pH 6.5 and 35 °C. The K_m and K_{cat} of NirK on sodium nitrite were 0.27 mM and 0.36×10^3 s^{-1}, respectively. Finally, homology model analysis of NirK indicated that the enzyme was a homotrimer structure and well conserved in Cu-binding sites for enzymatic functions. This is a first report for nitrite reductase from *Bacillus firmus*, which augment the acquaintance of nitrite reductase.

Keywords Cu-containing nitrite reductase · *Bacillus firmus* GY-49 · Gene expression · Enzyme activity

Introduction

Nitrite accretion was harmful to microbes and it can be reduced to nitric oxide (Ezzine and Ghorbel 2006). Denitrification was a process eliminates the nitrite accumulation in order to reduction of nitrate, nitrite, nitric oxide (NO) and nitrous oxide (N_2O) by nitrate reductase, nitrite reductase, NO reductase and N_2O reductase, respectively (Alvarez et al. 2014; Tiedje et al. 1988). Denitrifying bacteria are well represented among members of the genus *Bacillus* (Verbaendert et al. 2011). *Bacillus* was a classic envoy with not only the strong ability of water colonization and also environmental discharge safety, indicates that has a wide application in nitrogen pollution control (Mania et al. 2014).

Reduction of nitrite to nitric oxide using nitrite reductase was considered to be the rate limiting step in the denitrification process (Santoro et al. 2006). Two types of nitrite reductase with distinct molecular structures and prosthetic metal have been discovered as a copper nitrite reductase encoded by the nirK gene and cytochrome cd1-nitite reductase encoded by the nirS gene that was the key enzyme and forms the unique feature between denitrifies and nitrate reducers (Hoffmann et al. 1998). Denitrifying bacteria contain either *nirK* or *nirS* (Jones et al. 2008). The Cu-containing nitrite reductase (CuNiR) formed by *nirK* gene was distributed widely and molecular structure were studied well in denitrifying gram-negative bacteria (MacPherson and Murphy 2007; Lintuluoto and Lintuluoto 2016; Li et al. 2015; Ezzine and Ghorbel 2006; Berks et al. 1995). CuNiR contains type-1 Cu centre was bounded by two histidine, cysteine and methionine ligand, even as the indistinct tetrahedral type-2 Cu centre was corresponding by three histidine ligands and a single water molecule (Tocheva et al. 2004). The functionality of CU containing nitrite reductase shown in Fig. 1, NO_2^- eliminates water and transferred to the CuNIR of Cu(II) centre via its two oxygen atoms. Reduction

Electronic supplementary material The online version of this article (https://doi.org/10.1007/s11274-017-2383-6) contains supplementary material, which is available to authorized users.

✉ Nan Hu
hunan@njut.edu.cn

[1] College of Biotechnology and Pharmaceutical Engineering, Nanjing Tech Univerisity, Nanjing 211800, China

[2] State Key Laboratory of Agricultural Microbiology, College of Life Science and Technology, Huazhong Agricultural University, Wuhan 430070, China

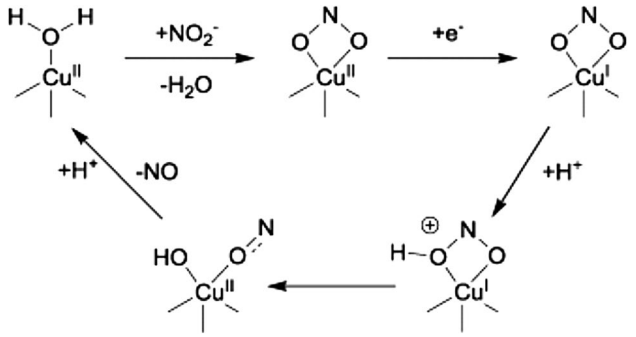

Fig. 1 The Mechanism of action of nitrite reduction in CuNIR. Source of the figure from Timmons and symes (2015)

of the Cu(II) centre, later on occurs as consequence of electron transfer from a Cu(I) centre, it's probably due to the stimulation of protonation with nearby aspartate residue. Sometimes, the bound nitrite was followed to protonated at the oxygen that is to be distracted, subsequently lysis of N–OH bond. After the N–OH was broken, protonation of the Cu-OH and it leads to NO discharge subsequently formation of a Cu(II)–H_2O composite. Later the water composite can be able to re-enter into catalytic system and perform its function in the reduction of nitrite (Timmons and Symes 2015). Fukuda et al. 2011 reported molecular and structure analysis of CuNiR in Gram-positive bacteria of *Geobacillus kaustophilus* HTA426. However, the report didn't show the enzyme characteristics of CuNiR in *Bacillus*. Therefore, it is important to characterize CuNiR in *Bacillus*.

In the present study *Bacillus firmus* GY-49 was isolated from the natural environment and it showed denitrification of nitrate as terminal electron acceptor. Here we have studied the biochemical properties of CuNiR encoded by the *nirK*-homolog gene, which is found in the *B. firmus* GY-49 genome The gene was cloned and expressed in *Escherichia coli*, and its molecular and catalytic properties characterized. Further, the structure of CuNiR was studied based on the sequence and structure analysis of well-known CuNiRs. The results showed that the *nirK* was really an ortholog of *nirK* in the denitrifying bacteria. This was the first report on the enzyme characteristics of CuNiR in *B. firmus*.

Materials and methods

Strains and plasmids

Bacillus firmus GY-49 (GenBank: KF982018.1) have been used to amplify the *nirK* gene. The *E.coli* strains DH5α and BL21 (DE3) (Invitrogen Co. Ltd., Shanghai, China) were employed for recombinant plasmid construction of the *nirK* gene. The pMD-19T vector (TaKaRa Biotechnology Co. Ltd., Dalian, China) and pET-28a (+) plasmid (Novagen Co. Ltd., Shanghai, China) were used for gene cloning and heterologous expression of *nirK* in *E. coli* BL21 (DE3).

Cloning and construction of recombinet vector

The specific primers for PCR amplification were designed based on gene encoding the putative nitrite reductase genome information of *B. firmus* GY-49. The putative protein was encoded by 353 amino acids and the N-terminal region from Met1 to Ala26 was considered to be a signal sequence analyzed by SignalP 4.1, which can predict the location of signal peptide cleavage sites in amino acid sequences (http://www.cbs.dtu.dk/services/SignalP/) (Emanuelsson et al. 2007). The *nirK* gene without signal peptide was amplified with the following primers *nir*K F: 5′-CCG *GAATTC*ATGCCGGAAAATTCCCTTCA-3′ and *nirK* R: 5′-CCC*AAGCTT*TTAATGGCTCATTGTAGCCT-3′ with restriction enzyme sites of *Eco*RI and *Hin*dIII, (Italics). PCR was performed in a thermal cycler programmed with 5 min at 94 °C, 30 s at 94 °C, 30 s at 50 °C, 100 s at 72 °C, and a final elongation 10 min at 72 °C. Then full-length gene was cloned into pMD19T, followed to transform into DH5α and obtained *nirK*-PCR.

The purified fragment of *nirK*-PCR was ligated to the pET28a (+) expression vector at corresponding restriction sites and obtained expression vector pET-NirK. To ensure the recombinant protein could express as expected, a Met residue was inserted prior to N-terminus (before the Phe27 residue of NirK). The Phe residue was quoted as first amino acid of the recombinant protein for subsequent clarity. The pET-NirK was transformed into the *E. coli* BL21 (DE3) competent cells for expression. A final concentration of 0.1 mM isopropyl-β-d-thiogalactoside and 1 mM CuSO4 for the activation of the recombinant protein was added when the optical density at 600 nm (OD600) reached 0.5. To acquire the functional version of cells were further incubated at 4 °C for 72 h after induction at 16 °C for 4 20 h. Next, the cells were collected and washed twice with PBS buffer (0.8% NaCl, 0.02% KCl, 0.142% Na2HPO4, 0.027% KH2PO4; pH 7.4) by centrifugation at 8000 rpm for 10 min and resuspended in PBS buffer and then the cells were disrupted by a French press and the crude enzyme was obtained as supernatant by centrifugation at 12,000 rpm for 40 min at 4 °C, followed to filtration by 0.22 μm filter membrane. The crude enzyme and the precipitation of insoluble protein were used for SDS–PAGE analysis.

Purification of the recombinant protein

The crude enzyme was loaded into Ni–NTA column (QIAGEN, China) pre-equilibrated in ten column volumes of 20 mM Tris–HCl buffer (pH 7.4) containing 250 mM

sodium chloride and 1 mM phenylmethylsulfonyl fluriode (buffer A). Then column was washed with five column volumes of same buffer A containing 20 mM imidazole and the buffer A containing 200 mM imidazole was applied to elute the recombinant protein. The fractions containing NirK were analyzed by SDS–PAGE.

In vitro activity assay for purified recombinant protein

Nitrite reductase activity was determined by using methyl viologen (MV) as an electron donor described by Abraham et al. 1993. The reaction was carried out (0.5 mL) in the closed vial containing 100 mM potassium phosphate buffer (pH 6.5), 50 mM methyl viologen and 2.5 M sodium nitrite, 1 M sodium chloride and 0.02 mL purified enzyme (Kataoka et al. 2000). The reaction was initiated with the addition of 50 µL sodium dithionite (1 M) and it was gently swirled. After incubation for 10 min at 37 °C, the reaction was terminated by vigorous shaking for 3 min. The rest of nitrite was determined by spectrophotometrically using diazo-coupling method of Nicholas and Nason (1957). One unit of activity corresponded to the reduction of 1 µmol of nitrite per minute.

Enzyme characterization

The optimum pH was determined by incubating the purified NirK at 35 °C in potassium phosphate buffer (5.7–8.0). The nitrite reductase activity was assayed by incubating 30 µL of enzyme solution in 50 µL of different pH buffers containing sodium nitrite at 35 °C for 10 min. For the effect of temperature, the activities of NirK was determined at different temperatures ranging from 20 to 60 °C. To study its thermostability, the enzyme was incubated at various temperatures (40, 45, 50, and 55 °C) in different time intervals (0–120 min). The enzyme stablility at different pH and temperatures were determined by measuring the residual activity of NirK in potassium phosphate buffer (pH 6.5) at 35 °C for 10 min.

The effects of metal ions and inhibitory additives were determined by pre-incubating the enzyme with 5 mM solution of the following Na^+, K^+, Cu^{2+}, Ba^{2+}, Mg^{2+}, Zn^{2+}, Mn^{2+}, Sr^{2+} and EDTA (ethylenediaminetetraacetic acid) and PMSF (phenylmethanesulfonyl fluoride) for 10 min to determine the residual activity. The nitrite reductase activity without additives was defind as 100%.

The kinetic properities of NirK were determined in the potassium phosphate buffer (pH 6.5) with different concentration of sodium nitrite at 35 °C for 10 min. The K_m and V_{max} values were calculated with Graphpad Prism software (Graphpad, San Diego, CA) according to non-linear regression plot using Michaelis–Menten equation. The k_{cat} was determined by the equation $k_{cat} = V_{max}/[E]$. All the assays were carried out in triplicate and against a control assay without enzyme.

Properties of absorption and structural modeling

Spectroscopic measurements were performed in the UV–visible regions using 220A Spectrophotometer (Lambda 25, Perkin Elmer, America) with a 1-cm long light path cuvette. According to Fukuda et al. (2011) and Arnold et al. (2006) structural modeling of NirK amino acid sequence without signal peptide was predicted on the Swiss-Model workspace to build a structure from *G. kaustophilus* (Accession No. 56419302).

Others

The protein concentration was determined by a modified lowry method using bovine serum albumin as the standard (Dulley and Grieve 1975). Amino acid sequences alignment was performed with the ClustalW program (Thompson et al. 1994). The complete cDNA sequence of nirK in *B. firmus* GY-49 has been submitted to GenBank database (Accession No. KT899614).

Results

Cloning and sequence analysis of *nirK* gene

The nucleotide sequence of *B. firmus* GY-49 was revealed the presence of an open reading frame of 1062-bp encoding CuNiR, composed of 353 amino-acid residues with a signal peptide. The full-length 993-bp cDNA of *nirK* without signal peptide was obtained through amplification (Figure not shown). The molecular weight of the recombinant protein was 36.41 kDa and predicted isoelectric point (pI) was 5.35. The amino acid sequence of NirK has highest similarity 99 and 78% with *B. firmus* and *Geobacillus stearothermophilus* in the NCBI.

Multiple sequence alignment showed T1Cu was integrated in each monomer and coordinated by four amino acid chains (two His imidazoles, one Cys thiolate and one Met thioether). The T_1Cu and T_2Cu was coordinated with two monomers and harmonized by three amino acid chains (two His imidazoles and one His imidazole from one subunit and the adjacent subunit, respectively). The two Cu sites at a distance of 12.5 Å, but are connected via the His-Cys sequence segment composed of the Cys residue of T_1Cu and His residue of T_2Cu (Godden et al. 1991). The amino acid sequence of NirK showed high identity to other well-known CuNiRs (Fig. 2). As shown in Fig. 2,

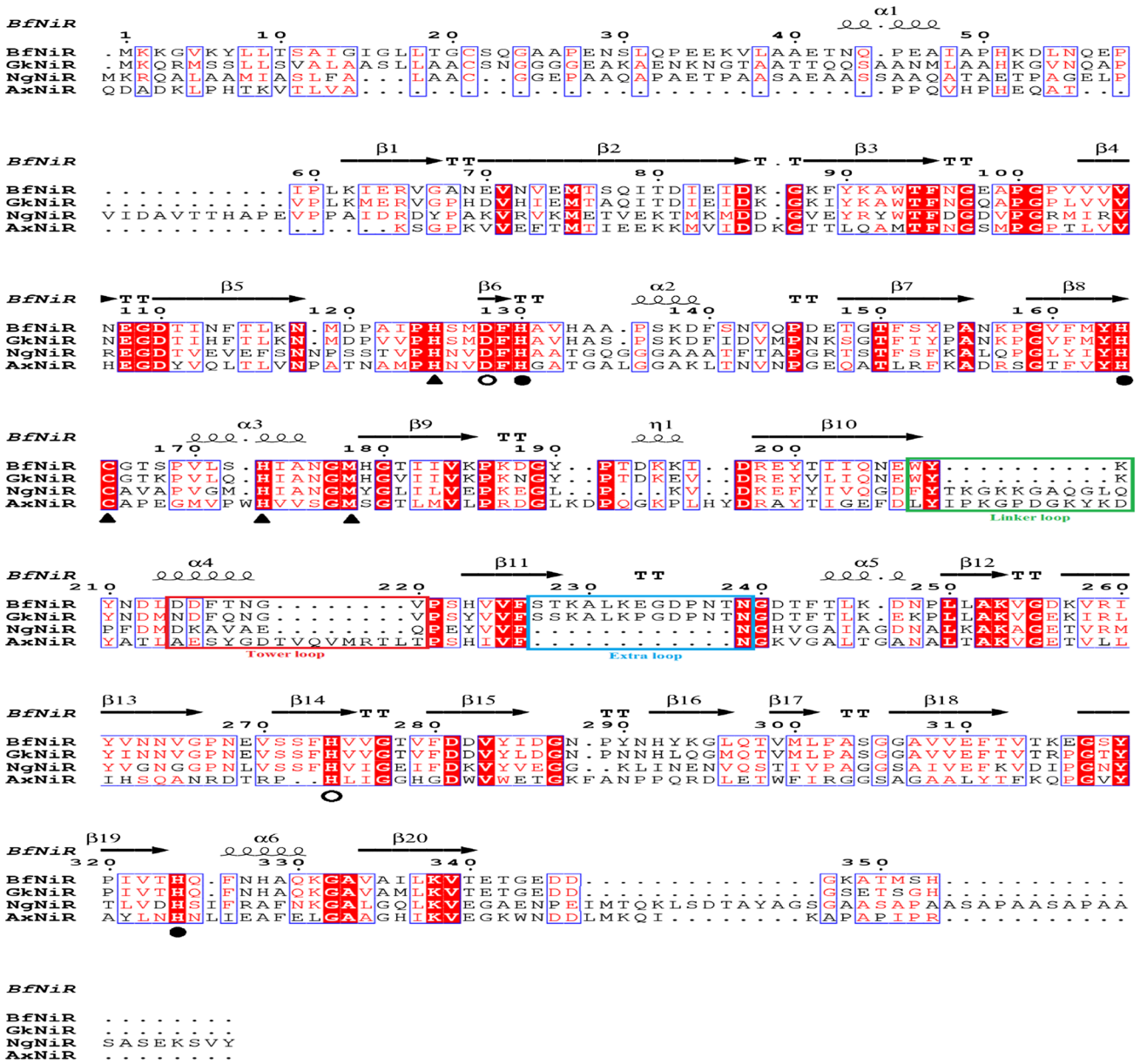

Fig. 2 Alignment of amino-acid sequences of CuNiR from different bacterial sources. The red section represents amino acid identity, and the similar amino acid including aromatic amino acid, basic amino acid, acidic amino acid, and hydrophobic acids. The filled triangle and circles under the sequence alignment signify the T_1Cu and T_2Cu ligands, respectively. The sequence for CuNiR was aligned with the following proteins (Accession numbers KT899614, Q5L1×8, 1KBWA, 1HAUA); Open circles indicate amino acid residues involved in a hydrogen bonding network around T_2Cu. The putative linker, loop tower and extra loop regions are in the box. The amino acid alignment was performed by *Clustal-W* package and the figure was generated using the program ESPript (Abraham et al. 1997; Gouet et al. 1999; Ladunga 2002)

these amino-acid sequences have been exposed that obvious conserved domain between each well-known CuNiR. The present results were agreed with previous studies of renowned CuNiRs, which were conserved in the active site of T_1Cu and T_2Cu formed by His125, Cys165, His173 and Met178 and His130, His164 and His324 residues.

Expression and purification of *nirK* gene

The CuNiR from *B. firmus* GY-49 was successfully expressed heterologously in *E. coli* BL21 (DE3) and the recombinant protein was purified by Ni^{2+}-NTA affinity chromatography. The CuNiR was analyzed by SDS–PAGE

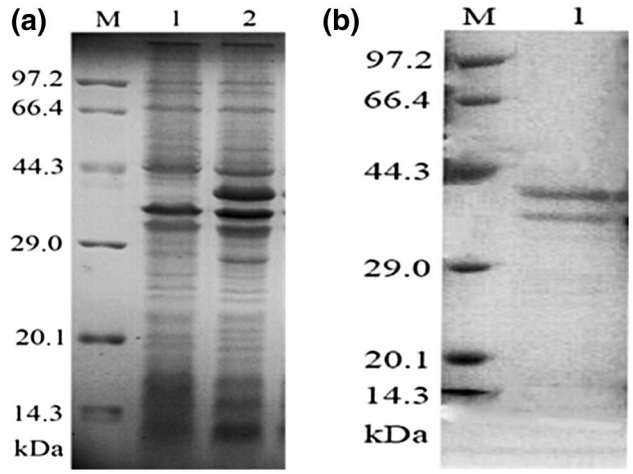

Fig. 3 **a** SDS-PAGE analysis of the recombinant crude enzyme. M: The protein molecular weight marker; Lane 1 The crude enzyme of recombinant strain *E. coli* BL21 (DE3) with pET-28a (+) as control; Lane 2 The crude enzyme recombinant strain *E. coli* BL21 (DE3) with pET-28a-NirK, **b** SDS-PAGE gel of the purified recombinant enzyme. Lane 1 Purified recombinant protein

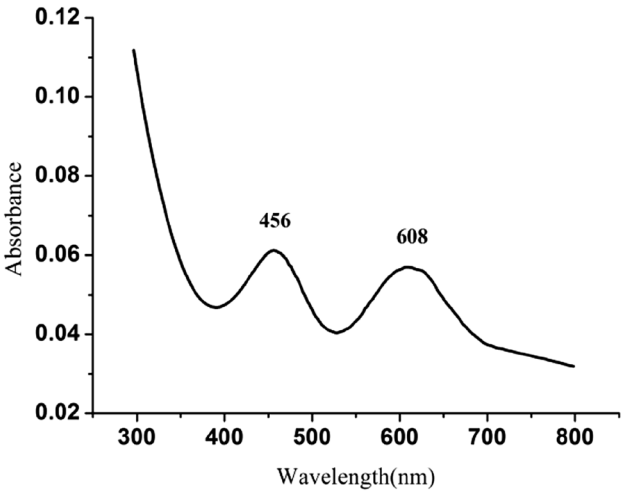

Fig. 4 UV and visible absorption spectrum of recombinant nitrite reductase. Purified NirK (0.91 mg/mL) was dissolved in 20 mM Tris–HCl buffer (pH 8.0) at room temperature. The absorbance of the enzyme at around 280 nm was reduced to a scale of 1/10 the natural intensity

(Fig. 3). The Fig. 3a showed a band of crude enzyme with molecular weight of approximately 37 kDa (amino acid sequences of the mature protein). The purified CuNiR was appeared two protein bands whose molecular weights to be 37 and 34 kDa with an approximately 1:1 stoichiometry, as shown in Fig. 3b.

Characterization of purified recombinant protein.

The purified enzyme appears bluish green in oxidized state and it becomes lighter color in reduction with $Na_2S_2O_4$, indicates presence of T_1Cu in the recombinant enzyme. The absorbance spectrum displayed two peaks at 456 and 608 nm in the spectrum of the visible region in Fig. 4. Similarly, the enzyme produced by *Nitrosococcus oceani* was showed two absorption peaks at 455 and 575 nm (Kondo et al. 2012).

Optimum pH, temperature and metal ions

Nitrite reductase activity was measured by using MV and sodium nitrite act as an electron donor and substrate. More prominently the amalgamation of Cu ions was essential for increasing enzyme activity since Cu ions could contribute to the reconstruction of T_2Cu (Kondo et al. 2012; Prudencio et al. 1999). The optimum pH of NirK was found to be at 6.5 and exhibited 93 and 78% of its retaining activity at 5.7 and 8.0, respectively (Fig. 5). Purified NirK showed broad activity range of a temperature from 20 to 60 °C (Fig. 6a). The enzyme showed maximum activity at 35 °C and retained more than 83 and 41% activity at 20 and 60 °C. In order to further study, the thermostability was studied in the range of a temperature from 40 to 55 °C (Fig. 6b). After 2 h incubation, NirK could retain more than 89.7% activity at 40 °C, but only about 24.35% activity was retained at 50 °C. However, it was almost inactive after 2 h incubation at 55 °C. The results showed that the enzyme has high catalytic efficiency at standard temperature, but it would become unstable at high temperatures. The purified recombinant protein had a specific activity of 98.4 U/mg in the periplasmic fraction under the optimal conditions. The present results were agreed with the existing of previous reports (Hira et al. 2012; Prudencio et al. 1999). In case of metal ions Na^+, Mg^{2+}, Mn^{2+}, Cu^{2+}, Sr^{2+} showed increase the activity of NirK by 3.26–34.91% (Table 1). NirK was less affected and retained about 89.09% of the original activity with certain concentration of Ba^{2+}, but it could inhibited by same concentration of Zn^{2+}. Interestingly, NirK was not sensitive to inhibitory additives (EDTA and PMSF) and it exhibits more than 80% activity (Table 1).

Kinetic studies

NirK kinetic parameters, K_m and K_{cat} were studied under standard method and conditions at pH 6.5 and 35 °C. The values of K_m and K_{cat} were 0.27 mM and 0.36×10^3 s^{-1}, respectively (Fig S1). The catalytic efficiency of NirK could be counted by K_m/K_{cat} with a computed value of 1.3×10^3 s^{-1} mM^{-1}. The present *Km* values were similar to a green-type of NirK from *Alcaligenes faecalis* and

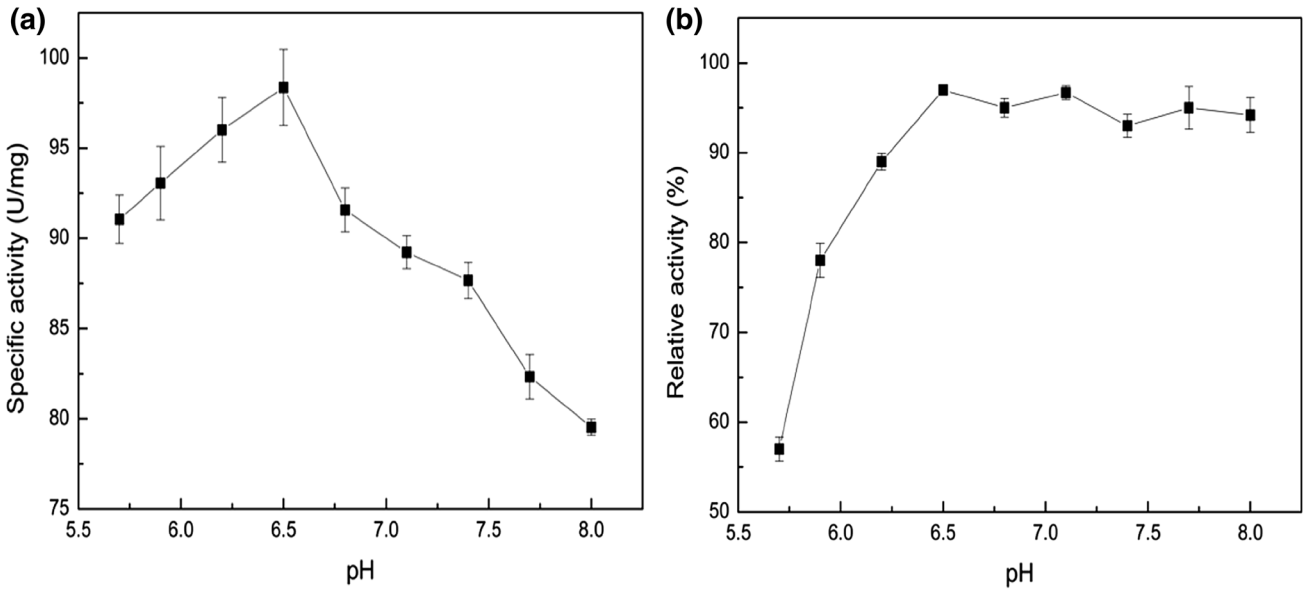

Fig. 5 The optimal pH and stability of the recombinant NirK. **a** The effect of pH on NirK activity. The activity was assayed at 35 °C in buffers containing a pH range of 5.7–8.0. **b** The effect of pH on the stability of NirK. The activity was measured under the standard procedure after the enzyme was incubated in different pH buffers at 35 °C for 2 h. Each value represents the average of triplicate experiments. Errors bars represent the standard deviation

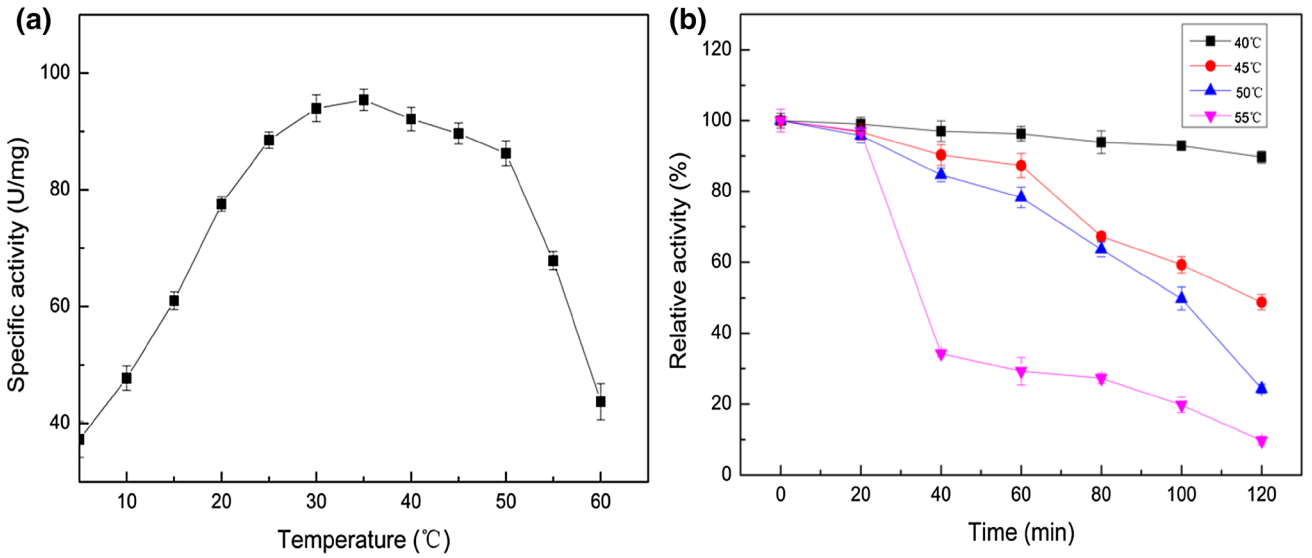

Fig. 6 The optimal temperature and stability of the recombinant NirK. **a** The effect of temperature on NirK activity. The activity was assayed at pH 6.5 at 20–60 °C. **b** The effect of temperatrue on the stability of NirK. The activity was measured under the standard procedure after the enzyme was incubated at 40, 45, 50, 55 °C in different time intervals and the residual activity was measured according to the standard conditions. Each value represents the average of triplicate experiments. Errors bars represent the standard deviation

sinorhizobium meliloti 2011 (Kukimoto et al. 1994; Ferroni et al. 2014).

Structural evolution

The structural modeling of CuNiR from *B. firmus* GY-49 was build with the *G. kaustophilus* nitrite reductase as template. The overall structure for NirK in *B. firmus* GY-49 could be folded into two cupredoxin domains of the

Table 1 Effects of various metal ions and inhibitory additives on NirK

Compound	Concentration (mM)	Relative activity (%)
None	–	100
Mn^{2+}	5	129.09 ± 1.9
Cu^{2+}	5	118.27 ± 2.7
Mg^{2+}	5	109.78 ± 2.1
Na^{2+}	5	134.91 ± 2.7
Sr^{2+}	5	103.26 ± 4.3
Ba^{2+}	5	89.09 ± 3.8
Zn^{2+}	5	76.27 ± 5.4
EDTA	5	81.2 ± 7.8
PMSF	5	87.23 ± 4.6

Data was shown as mean values ± SD. Various metal ions and other chemical compounds were added into the reaction mixture to a final concentration of 5 mM. The activity was determined at pH 6.5 and 35 °C. The enzyme activity without any additives was defined as 100%. All determinations were performed in triplicate

well-known CuNiR structure and each monomer consist of α-helix, β-pleated sheet and random helix. Generally, these conserved residues (H125, H173, C164, M178, H164, H130, H324, H274, D128) shown as firewood in Fig. 7a, were hypothetically to create the active catalytic sites of NirK. The confirmed structure was located in the southern surface of T_1Cu and functioned as the form of α-helix structure (Fig. 7a). In addition to that space occupied by the structure was corresponding to the interaction surface with the physiological redox-partner proteins (Nojiri et al. 2009). Previously reported structure analysis of *G. kaustophilus* suggested that the N-terminal α-helix could play an important role for effective electron transfer in physiological redox-partners pairs (Fukuda et al. 2014). However, similar residues composed of N-terminal α-helix in *B. firmus* GY-49 are shorter than those in *G. kaustophilus*, which is colored in gray (Fig. 7b). Superimposing the predicted structure of CuNiR from this study on the established for comparison,

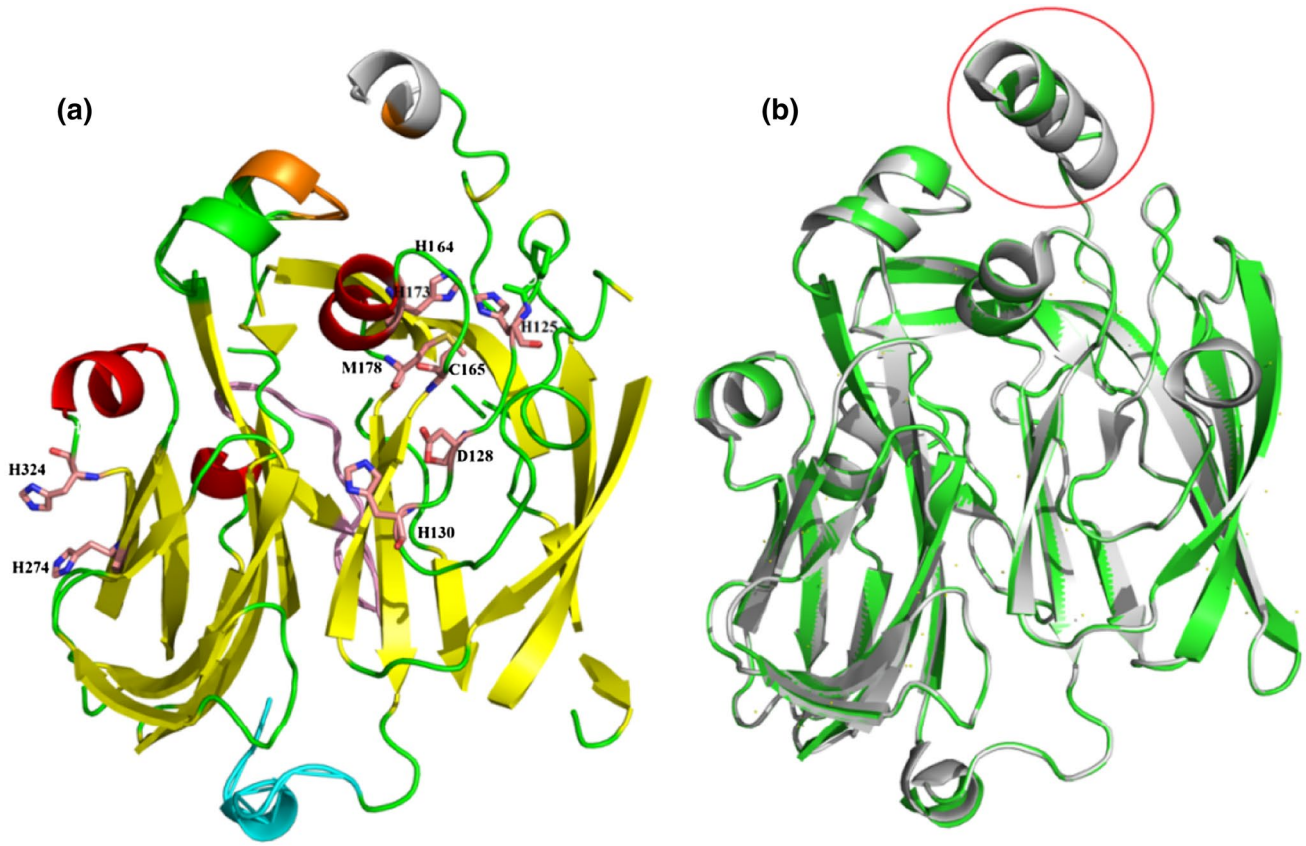

Fig. 7 Homology modeling of the NirK structure. Homology modeling of NirK from *G. kaustophilus*. **a** Protein secondary structure showed α-helix, β-pleated sheet and random coil were colored by red, yellow and blue, respectively. In particularly residues (H125, H173, C164, M 178, H164, H130, H324) are involved in the formation of T1Cu and T_2Cu site of NirK. Moreover, the "Linker", "Tower" and "Extra" loops are colored by blue, orange and pink, respectively. N-terminal region formed α-helix structure is signed by light-gray and the dashed-line circle indicates the space occupied by the N-terminal region in other well-known CuNiRs. This figure was generated using the PYMOL program (DeLano 2002). **b** Superimpose of the CuNiR from *B. firmus* GY-49 (green) and *G. kaustophilus* (gray). The structure of the main chain is almost the same between the two structures. The red line represents the difference in α-helix structure between two *Bacillus* groups

lead to following observations. N-terminal region of the T1Cu and overall structure of CuNiR from *B. firmus* GY-49 were well relation with tertiary structure of CuNiR from *G. kaustophilus*. Moreover it shows that there is no connection between the folding of the core region of CuNiR and length of N-terminal region in the *B. firmus* GY-49. The results implied that the novel structure may be existing in CuNiR in all *Bacillus*, which may be the subject of further attempts at crystallizing the enzyme.

Discussion

To date, CuNiR produced by *B. firmus* was the first report and it belongs to Gram-positive bacteria. The literature showed only one eminent CuNiR from *G. kaustophilus* HTA426 (Fukuda et al. 2011) which was functionally verified and present results showed 72.73% similarity. All CuNiRs has trimeric structure and each monomer consisted of two types of Cu that plays a very important role in catalysis, which was defined as type 1 (T_1Cu) and type 2 (T_2Cu), respectively. Generally the active site of T_1Cu could accept an electron from external electron transfer protein and was accepted by T_2Cu in electron transfer process of CuNiRs (Iwasaki et al. 1975; Kakutani et al. 1981).

Hira et al. (2012) reported that formation of T_1Cu by His122, Cys159, His168 and Met173 conserved sequence and His127, His158 and His321 for T_2Cu in Anammox organism KSU-1. In addition Asp128 and His274 were identified in the sequence of CuNiR, suspecting that these residues may involve forming hydrogen bond during proton transform to NO^-. The SDS–PAGE analysis showed two bands, in which second lower band was probably a degradation product of the larger subunit was similar to other nitrite reductase (Inatomi and Hochstein 1996; Rosa et al. 2001). The present results were related with previous report of Suzuki et al. 1999. Based on the T_1Cu absorption characteristics CuNiRs has been divided into green and blue enzyme. This was due to the geometrical distortion of the T_1Cu (LaCroix et al. 1996). In contrast to the nitrite reductase from *Alcaligenes xylosoxidans* showed a single absorption peak at 595 nm indicates blue enzyme (Prudencio and Sawers 1999). As well as the ratio (A455/A608) of NirK from *anammox* bacterium KSU-1 and *A.faecalis* was 1.03 which was reasonable to NirK (Wijma et al. 2006). The results implied that the CuNiR from *B. firmus* GY-49 resemble that green-type nitrite reductase belong to class II (Kobayashi and Shoun 1995; Suzuki et al. 1999; Leferink et al. 2012; Nojiri et al. 2009; Hoffmann et al. 1998).

Moreover CuNiR can be divided into two distinct groups, class-I and Class-II (Boulanger and Murphy 2002). A characteristic difference between the class I and class II groups was the length of the linker loop and tower loop. The tower loop in class I CuNIRs extends to the upper surface of the type 1 Cu site and was important for docking with the electron transfer partners. There are partial deletions in the linker loop and tower loop of class II (Boulanger and Murphy 2002). Sequence alignment analysis of NirK from *B. firmus* GY-49 showed linker loops and tower loops of Class-II CuNiR were shorter than those found in Class-I CuNiR. Interestingly, the Class-II CuNiR from *B. firmus* GY-49 and *G. kaustophilus* exhibited similar characteristics of linker loops and tower loops, its due to the related or close physiological and genetic relationship between these two Gram-positive bacterium. Furthermore a distinctive extra loop was found in *B. firmus* GY-49 as well as in *G. kaustophilus*. The extra loop consisted of 12 residues were located in the N-terminal region of CuNiRs (Fukuda et al. 2014). Likewise presents of N-terminal region (extra loop) in *B. firmus* GY-49 was a novel and unique structure for Gram-positive bacteria. Moreover the interaction and electron transfer mechanisms for CuNiR and relevant physiological electron donor protein was well studied in denitrifying bacteria (Dodd 1995; Kabayashi and Shoun 1995; Liu et al. 1986). The physiological electron donor of CuNiR from *B. firmus* GY-49 could not be defined, However, it is worth mentioning that we have found the presence of Cytochrome c551 instead of pseudoazurin or azurin analogues in the genome of the B. firmus GY-49. Therefore CuNiR protein acts as a physiological electron-donor between the electron transfer reactions through its acidic residues located around the T_1Cu site. In order to confirm the above statement, further research was continued about mechanism of action of NirK.

Conclusion

The spectroscopic and molecular properties of the enzyme imply that NirK is a green-type CuNiR. Predominantly, the recombinant enzyme displayed a higher activity than those in the *G. kaustophilus* HAT426, and the enzyme was a moderate and organic solvents tolerant reductase with remarkable stability, it was proposed to be a potential microecologics for wastewater treatment. Furthermore, homology analysis of CuNiR in *B. firmus* GY-49 shown a few new characteristics, including extra loop and N-terminal α-helix around the T_1Cu site. CuNiR possessed an N-terminal α-helix, which can greatly contribute to the interaction between the partner protein and CuNiR. The present results of the CuNiR have great value to the application of nitrite reduction in polluted water.

References

Abraham ZH, Lowe DJ, Smith BE (1993) Purification and characterization of the dissimilatory nitrite reductase from *Alcaligenes xylosoxidans* subsp. xylosoxidans (N.C.I.M.B. 11015): evidence for the presence of both type 1 and type 2 copper centres. Biochem J 295:587–593. https://doi.org/10.1264/jsme2.ME11310

Abraham ZHL, Smith BE, Howes BD, Lowe DJ, Eady RR (1997) pH dependance for binding a single nitrite ion to each type-2 Cu center in the Cu-containing nitrite reductase of *Alcaligenes xylosoxidans*. Biochem J 324:511–516

Alvarez L, Bricio C, Blesa A, Hidalgo A, Berenguer J (2014) Transferable denitrification capability of *Thermus thermophilus*. Appl Environ Microbiol 80:19–28. https://doi.org/10.1128/AEM.02594-13

Arnold K, Bordoli L, Kopp J, Schwede T (2006) The SWISS-MODEL Workspace. A web-based environment for protein structure homology modelling. Bioinformatics 22:195–201. https://doi.org/10.1093/bioinformatics/bti770

Berks BC, Ferguson SJ, Moir JW, Richardson DJ (1995) Enzymes and associated electron transport systems that catalyse the respiratory reduction of nitrogen oxides and oxyanions. Biochim Biophys Acta 1232:97–173. https://doi.org/10.1016/0005-2728(95)00092-5

Boulanger MJ, Murphy ME (2002) Crystal structure of the soluble domain of the major anaerobically induced outer membrane protein (AniA) from pathogenic Neisseria: a new class of copper-containing nitrite reductase. J Mol Biol 315:1111–1127

DeLano WL (2002) The PyMOL molecular graphics system. De Lano Scientific, San Carlos. http://www.pymol.org/

Dodd FE (1995) Evidence for two distinct azurins in *Alcaligenes xylosoxidans* (NCIMB 11015): potential electron donors to nitrite reductase. Biochemistry 34:10180–10186. https://doi.org/10.1021/bi00032a011

Dulley JR, Grieve PA (1975) A simple technique for eliminating interference by detergents in the lowry method of protein determination. Anal Biochem 64:136–141. https://doi.org/10.1016/0003-2697(75)90415-7

Emanuelsson O, Brunak S, Heijne G, Nielsen H (2007) Locating proteins in the cell using TargetP, SignalP and related tools. Nat Protoc 2:953–971. https://doi.org/10.1038/nprot.2007.131

Ezzine M, Ghorbel MH (2006) Physiological and biochemical responses resulting from nitrite accumulation in tomato (*Lycopersicon esculentum* Mill. cv. Ibiza F1). J Plant Physiol 163:1032–1039. https://doi.org/10.1016/j.jplph.2005.07.013

Ferroni FM, Marangon J, Neuman NI, Cristaldi JC, Brambilla SM, Guerrero SA, Rivas MG, Rizzi AC, Brondino CD (2014) Pseudoazurin from *Sinorhizobium meliloti* as an electron donor to copper-containing nitrite reductase: influence of the redox partner on the reduction potentials of the enzyme copper centers. J Biol Inorg Chem 19:913–921

Fukuda Y, Tamada T, Takami H, Suzuki S, Inoue T, Nojiri M (2011) Cloning, expression, purification, 3D-structure crystallization and preliminary X-ray crystallographic study of GK0767, the Cu-containing nitrite reductase from *Geobacillus kaustophilus*. Acta 3D-structurelogr F67:692–695. https://doi.org/10.1107/S1744309111013297

Fukuda Y, Koteishi H, Yoneda R, Tamada T, Takami H, Inoue T, Nojiri M (2014) Structural and functional characterization of the *Geobacillus* Cu nitrite reductase: Involvement of the unique N-terminal region in the interprotein electron transfer with its redox partner. Biochim Biophyc Acta 183:7396–7405. https://doi.org/10.1016/j.bbabio.2014.01.004

Godden JW, Turley S, Teller DC, Adman ET, Liu MY, Payne WJ, Gall JLe (1991) The 2.3 Å X-ray structure of nitrite reductase from *Achromobacter cycloclastes*. Science 253:438–442. https://doi.org/10.1126/science.1862344

Gouet P, Courcelle E, Stuart DI, Metoz F (1999) ESPript: analysis of multiple sequence alignments in PostScript. Bioinformatics 15:305–308

Hira D, Toh H, Migita CT, Okubo H, Nishiyama T, Hattori M, Furukawa K, Fujii T (2012) Anammox organism KSU-1 expresses a NirK-type copper-containing nitrite reductase instead of a NirS-type with cytochrome cd1. 586(11):1658–1663. https://doi.org/10.1016/j.febslet.2012.04.041

Hoffmann T, Frankenberg N, Marino M, Jahn D (1998) Ammonification in *Bacillus subtilis* utilizing dissimilatory nitrite reductase is dependent on resDE. J Bacteriol 180:186–189

Inatomi K, Hochstein LI (1996) The purification and properties of a copper nitrite reductase *Haloferax denitrificans*. Curr Microbiol 32:72–76. https://doi.org/10.1007/s002849900013

Iwasaki H, Noji S, Shidara S (1975) *Achromobacter cycloclastes* nitrite reductase. The function of Cu, amino acid composition, and ESR spectra. J Biochem 78:355–361

Jones CM, Stres B, Rosenquist M, Hallin S (2008) Phylogenetic analysis of nitrite, nitric oxide, and nitrous oxide respiratory enzymes reveal a complex evolutionary history for denitrification. Mol Biol Evol 25(9):1955–1966. https://doi.org/10.1093/molbev/msn146

Kabayashi K, Shoun H (1995) The copper-containing dissimilatory nitrite reductase involved in the denitrifying system of the fungus *Fusarium oxysporum*. J Biol Chen 270:4146–4151

Kakutani TH, Watanabe H, Arima K, Beppu T (1981) Purification and properties of a Cu-containing nitrite reductase from a denitrifying bacterium *Alcaligenes faecalisstrain* S-6. J Biochem 89:453 – 46

Kataoka K, Furusawa H, Takagi K, Yamaguchi K, Suzuki S (2000) Functional analysis of conserved aspartate and histidine residues located around the type 2 Cu site of Cu-containing nitrite reductase. J Biochem 127:345–350

Kobayashi M, Shoun H (1995) The Cu-containing dissimilatory nitrite reductase involved in the denitrifying system of the fungus *Fusarium oxysporum*. J Biol Chem 270:4146–4151

Kondo K, Yoshimatsu K, Fujiwara T (2012) Expression, and molecular and enzymatic characterization of Cu-containing nitrite reductase from a marine ammonia-oxidizing gammaproteobacterium, *Nitrosococcus oceani*. Microbes Environ 27:407–412. https://doi.org/10.1264/jsme2.ME11310

Kukimoto M, Nishiyama M, Murphy MEP, Turley S, Adman ET, Horinouchi S, Beppu T (1994) X-ray structure and site-directed mutagenesis of a nitrite reductase from *Alcaligenes faecalis* S-6: roles of two copper atoms in nitrite reduction. Biochemistry 33:5246–5252

Ladunga I (2002) Finding homologs to nucleotide sequences using network BLAST searches. Curr Protoc Bioinform. https://doi.org/10.1002/0471250953.bi0303s00

LaCroix LB, Shadle SE, Wang Y, Averill BA, Hedman B, Hodgson KO, Solomon EI (1996) Electronic structure of the perturbed blue copper site in nitrite reductase: a spectroscopic properties, bonding, and implications for the entatic/rack state. J Am Chem Soc 118:7755–7768

Leferink NG, Pudney CR, Brenner S, Heyes DJ, Eady RR, Samar Hasnain S, Hay S, Rigby SE, Scrutton NS (2012) Gating mechanisms for biological electron transfer: Integrating structure with biophysics reveals the nature of redox control in cytochrome P450 reductase and Cu-dependent nitrite reductase. FEBS Lett 586:578–584. https://doi.org/10.1016/j.febslet.2011.07.003

Li Y, Hodak M, Bernholc J (2015) Enzymatic mechanism of copper-containing nitrite reductase. Biochem 54:1233–1242. https://doi.org/10.1021/bi5007767

Lintuluoto M, Lintuluoto JM (2016) DFT study on nitrite reduction mechanism in copper-containing nitrite reductase. Biochem 55:210–223. https://doi.org/10.1021/acs.biochem.5b00542

Liu MY, Liu MC, Payne WJ, Legall J (1986) Properties and electron transfer specificity of copper proteins from the denitrifier "*Achromobacter cycloclastes*". J Bacteriol 166:604–608

MacPherson IS, Murphy ME (2007) Type-2 Cu-containing enzymes. Cell Mol Life Sci 64:2887–2899

Mania D, Heylen K, van Spanning RJ, Frostegard A (2014) The nitrate-ammonifying and *nosZ*-carrying bacterium *Bacillus vireti* is a potent source and sink for nitric and nitrous oxide under high nitrate conditions. Environ Microbiol 16:3196 – 210. https://doi.org/10.1111/1462-2920.12478

Martinez-Espinosa RM, Marhuenda-Egea FC, Bonete MJ (2001) Purification and characterization of a possible assimilatory nitrite reductase from the halophile archaeon *Haloferax mediterranei*. FEMS Microbiol Lett 196:113–118. https://doi.org/10.1111/j.1574-6968.2001.tb10550.x

Nicholas DJD, Nason A (1957) Determination of nitrate and nitrite. Methods Enzymol 3:981–984

Nojiri M, Koteishi H, Nakagami T, Kobayashi K, Inoue T, Yamaguchi K, Suzuki S (2009) Structural basis of inter-protein electron transfer for nitrite reduction in denitrification. Nature 462:117–120. https://doi.org/10.1038/nature08507

Prudencio M, Eady RR, Sawers G (1999) The blue copper-containing nitrite reductase from *Alcaligenes xylosoxidans*: cloning of the nirA gene and characterization of the recombinant enzyme. J Bacteriol 181:2323–2329

Santoro AE, Boehm AB, Francis CA (2006) Denitrifier community composition along a nitrate and salinity gradient in a coastal aquifer. Appl Environ Microbiol 72:2102–2109. https://doi.org/10.1128/AEM.72.3.2102-2109.2006

Suzuki S, Kataoka K, Yamaguchi K, Inoue T, Kai Y (1999) Structure function relationships of Cu-containing nitrite reductases. Coord Chem Rev 190–192:245–265

Thompson JD, Higgins DG, Gibson TJ (1994) CLUSTALW: improving the sensitivity of progressive multiple sequence alignment through sequence weighting, position-specific gap penalties and weight matrix choice. Nucleic Acids Res 22:4673–4680

Tiedje JMZ (1988) Ecology of denitrification and dissimilatory nitrate reduction to ammonium. In: Zehnder AJB (ed) Environmental microbiology of anaerobes. Wiley, New York, pp 179–244

Timmons AJ, Symes MD (2015) Converting between the oxides of nitrogen using metal ligand coordination complexes. Chem Soc Rev 44:6708–6710

Tocheva EI, Rosell FI, Mauk AG, Murphy ME (2004) Side on copper nitrosyl coordination by nitrite reductase. Science 304:867–870

Verbaendert I, Boon N, De Vos P, Heylen K (2011) Denitrification is a common feature among members of the genus *Bacillus*. Syst Appl Microbiol 34:385–391. https://doi.org/10.1016/j.syapm.2011.02.003

Wijma HJ, Jeuken LJC, Verbeet MP, Armstrong FA, Canters GW (2006) A random-sequential mechanism for nitrite binding and active site reduction in copper-containing nitrite reductase. J Biol Chem 281:16340–16346